



# A model for malaria treatment evaluation in the presence of multiple species

C.R. Walker<sup>a,\*</sup>, R.I. Hickson<sup>a,b,c</sup>, E. Chang<sup>a</sup>, P. Ngor<sup>d,e</sup>, S. Sovannaroeth<sup>d</sup>, J.A. Simpson<sup>f</sup>,  
D.J. Price<sup>f,g</sup>, J.M. McCaw<sup>a,f</sup>, R.N. Price<sup>e,h,i</sup>, J.A. Flegg<sup>a</sup>, A. Devine<sup>f,h</sup>

<sup>a</sup> School of Mathematics and Statistics, University of Melbourne, Australia

<sup>b</sup> Australian Institute of Tropical Health and Medicine, and College of Public Health, Medical & Veterinary Sciences, James Cook University, Australia

<sup>c</sup> Health and Biosecurity, CSIRO, Australia

<sup>d</sup> Cambodian National Center for Parasitology, Entomology and Malaria Control, Cambodia

<sup>e</sup> Mahidol-Oxford Tropical Medicine Research Unit, Faculty of Tropical Medicine, Mahidol University, Thailand

<sup>f</sup> Centre for Epidemiology and Biostatistics, Melbourne School of Population and Global Health, University of Melbourne, Australia

<sup>g</sup> Department of Infectious Diseases, University of Melbourne, at the Peter Doherty Institute for Infection and Immunity, Australia

<sup>h</sup> Division of Global and Tropical Health, Menzies School of Health Research and Charles Darwin University, Australia

<sup>i</sup> Centre for Tropical Medicine and Global Health, Nuffield Department of Clinical Medicine, University of Oxford, UK

## ARTICLE INFO

Dataset link: <https://github.com/jnwalker2/multispecies-malaria-model>

### Keywords:

Malaria

Unified treatment

*Plasmodium falciparum*

*Plasmodium vivax*

Stochastic modelling

## ABSTRACT

*Plasmodium falciparum* and *P. vivax* are the two most common causes of malaria. While the majority of deaths and severe morbidity are due to *P. falciparum*, *P. vivax* poses a greater challenge to eliminating malaria outside of Africa due to its ability to form latent liver stage parasites (hypnozoites), which can cause relapsing episodes within an individual patient. In areas where *P. falciparum* and *P. vivax* are co-endemic, individuals can carry parasites of both species simultaneously. These mixed infections complicate dynamics in several ways: treatment of mixed infections will simultaneously affect both species, *P. falciparum* can mask the detection of *P. vivax*, and it has been hypothesised that clearing *P. falciparum* may trigger a relapse of dormant *P. vivax*. When mixed infections are treated for only blood-stage parasites, patients are at risk of relapse infections due to *P. vivax* hypnozoites.

We present a stochastic mathematical model that captures interactions between *P. falciparum* and *P. vivax*, and incorporates both standard schizonticidal treatment (which targets blood-stage parasites) and radical cure treatment (which additionally targets liver-stage parasites). We apply this model via a hypothetical simulation study to assess the implications of different treatment coverages of radical cure for mixed and *P. vivax* infections and a “unified radical cure” treatment strategy where *P. falciparum*, *P. vivax*, and mixed infections all receive radical cure after screening glucose-6-phosphate dehydrogenase (G6PD) normal. In addition, we investigated the impact of mass drug administration (MDA) of blood-stage treatment. We find that a unified radical cure strategy leads to a substantially lower incidence of malaria cases and deaths overall. MDA with schizonticidal treatment was found to decrease *P. falciparum* with little effect on *P. vivax*. We perform a univariate sensitivity analysis to highlight important model parameters.

## 1. Introduction

Almost half of the world’s population is at risk of malaria, with ongoing transmission reported in 85 countries (WHO, 2021). In 2020 there were an estimated 241 million cases and 627,000 malaria deaths, with funding for control and elimination estimated at US\$3.3 billion (WHO, 2021). Over the last decade substantial gains have been made in reducing the burden of disease. In 2014 the leaders of 18 malaria endemic countries in the Asia Pacific committed to eliminating the disease in the region by 2030 (Gosling et al., 2012). In this region the two parasite species that cause the greatest burden of malaria are

*Plasmodium falciparum* and *P. vivax*. Most research and intervention efforts have been focused on *P. falciparum*, the most pathogenic parasite species. However, outside of Africa *P. vivax* is becoming the predominant cause of malaria, and almost invariably co-exists with *P. falciparum*. While malaria control measures impact both species, these are often less effective against *P. vivax* primarily due to the parasite’s ability to form dormant liver parasites (hypnozoites) that can reactivate weeks to months after the initial infection, causing future infections (relapses). *P. vivax* also forms sexual stages early in infection and is able to transmit to the mosquito vector before the patient seeks treatment.

\* Corresponding author.

E-mail address: [camelia.walker@unimelb.edu.au](mailto:camelia.walker@unimelb.edu.au) (C.R. Walker).

<https://doi.org/10.1016/j.epidem.2023.100687>

Received 13 July 2022; Received in revised form 12 March 2023; Accepted 12 May 2023

Available online 18 May 2023

1755-4365/© 2023 Published by Elsevier B.V. This is an open access article under the CC BY-NC-ND license (<http://creativecommons.org/licenses/by-nc-nd/4.0/>).

Furthermore, *P. vivax*'s lower parasite density makes it more difficult to detect than *P. falciparum*.

Primaquine is the only widely-used drug available that kills hypnozoites. The combination of primaquine plus a schizonticidal drug, such as chloroquine (CQ) or artemisinin-based combination therapies (ACT), is known as radical cure. Primaquine can cause drug-induced haemolysis in individuals with glucose-6-phosphate dehydrogenase (G6PD) deficiency, an inherited enzymopathy present in up to 30% of malaria endemic populations. For this reason the WHO recommends screening for G6PD deficiency prior to administration of primaquine to reduce the risk of severe primaquine-induced haemolysis (WHO, 2022). The effectiveness of primaquine is limited by the reluctance of healthcare providers to prescribe it, and patient adherence to complete a course of treatment (Thriemer et al., 2017). New point-of-care tools for diagnosing G6PD deficiency have recently come onto the market but have yet to be introduced widely into clinical practice. The challenges of *P. vivax* control, including safely and consistently treating *P. vivax* with radical cure, have resulted in its relative rise as a proportion of malaria cases (Kenangalem et al., 2019; Price et al., 2020; Carrara et al., 2013). In one modelling study over 80% of *P. vivax* cases in the Greater Mekong Subregion (GMS) were estimated to have arisen from relapses (Adekunle et al., 2015), highlighting the importance of radical cure to reduce the burden of disease (Douglas et al., 2012).

Successful malaria elimination campaigns in co-endemic settings will require widespread use of safe and effective radical cure to patients presenting with *P. vivax* as well as the hidden reservoirs of infection. Failure to consider *P. vivax* malaria as a target for elimination may compromise *P. falciparum* elimination campaigns because communities that continue to experience cases of malaria, even if due to another type of parasite, may show a reduced willingness to participate in future interventions designed to prevent re-introduction of *P. falciparum*. In an effort to accelerate *P. falciparum* malaria elimination in the GMS, the use of mass drug administration (MDA) or mass screening and treatment is now being investigated (Landier et al., 2018). These interventions do not include radical cure, but all stages (blood and liver) of all parasite species will need to be eradicated to eliminate malaria. The GMS aims to eliminate all species of malaria by 2030. This prospect is complicated by the presence of *P. vivax* and mixed infections of both *P. falciparum* and *P. vivax*, which in some locations make up to 16.6% of malaria infections (Chhim et al., 2021).

Mixed infections can change treatment outcomes in several ways: a mixed infection will be treated for both species simultaneously, *P. falciparum* malaria can mask a *P. vivax* malaria co-infection (Abba et al., 2014; Ashton et al., 2010) and an episode of *P. falciparum* malaria is associated with a greater risk of *P. vivax* infection in the subsequent weeks after treatment (Commons et al., 2019; Lin et al., 2011; Hossain et al., 2020). It has been hypothesised that the fever and haemolysis caused by acute *P. falciparum* malaria may trigger reactivation of *P. vivax* hypnozoites and subsequent relapse. Whereas current practice reserves radical cure for patients presenting with *P. vivax* malaria, a unified treatment policy, in which patients presenting with either *P. vivax* or *P. falciparum* are prescribed radical cure, has potential to reduce recurrent episodes of malaria and target hidden reservoirs of infection (Poespoprodjo et al., 2022).

While a range of mathematical models for malaria have been proposed, implemented, analysed and used to support policy decisions over the last 100 years – as reviewed recently (Mandal et al., 2011; Smith et al., 2018) – few models have included the parasite dynamics of both *P. falciparum* and *P. vivax* (Aguas et al., 2012; Pongsumpun and Tang, 2008, 2010; Silal et al., 2019). To our knowledge, only one of these modelling investigations explored interactions between species (Silal et al., 2019). Silal et al. developed a deterministic metapopulation model of *P. falciparum* and *P. vivax*, and incorporated key interactions between *P. falciparum* and *P. vivax*, including “treatment entanglement” (any treatment affecting the other parasite species), “triggering” (*P. vivax* hypnozoite activation following an episode of *P. falciparum*),

and “masking” (where non-*P. falciparum* rapid diagnostic test (RDT) results are either missed or falsely attributed to be *P. falciparum*). The remaining models (Aguas et al., 2012; Pongsumpun and Tang, 2008, 2010) explicitly and/or effectively consider the dynamics of the two species to be completely independent.

We present the first stochastic agent-based model for the transmission of both *P. falciparum* and *P. vivax*, which addresses the dynamics of mixed infections, parasite interactions and antimalarial treatments. Our model considers humans as discrete agents which transition between compartments according to a continuous-time Markov chain (CTMC) model. The CTMC is coupled with a system of ordinary differential equations (ODEs) that govern the mosquito population, where the transmission rate both from mosquitoes-to-humans and humans-to-mosquitoes are held constant over small time-steps. The stochasticity of our model allows it to appropriately capture infectious disease dynamics at low incidence, as malaria approaches elimination. The model, however, does not explicitly consider non-treatment interventions. Our model has 6 compartments for *P. falciparum* and 7 for *P. vivax*, representing a model with lower complexity than the other multi-species model with interactions, which has 14 and 17 compartments, respectively (Silal et al., 2019). The reduction in model complexity partially comes from removing age-stratification from the model. One of the main effects of age is in the acquisition of immunity to prevent developing clinical malaria, which we capture through lower probabilities of clinical malaria upon reinfection or relapse (i.e., in the following, the probability of clinical malaria upon reinfection or relapse is 0.5, compared to 0.95 for a naive *P. falciparum* infection). Even with the reduction in model complexity compared to Silal et al. (2019), we note that our model requires many input parameters, many of which are poorly defined in the literature. Hence, we perform a univariate sensitivity analysis to understand the impact of changes to each parameter with respect to model output such as malaria cases and deaths.

As an example, we consider scenarios with a decreasing *P. falciparum* prevalence and a proportionally increasing *P. vivax* prevalence, which is representative of dynamics observed in some of the GMS and neighbouring areas (WHO, 2020). Our model is applied in a hypothetical simulation study to assess the effect of blood-stage treatment, differing coverage of radical cure prescription, and a unified treatment policy in which radical cure is prescribed to patients presenting with *P. vivax*, *P. falciparum*, and mixed infections. For each of these treatment scenarios, we also consider an MDA intervention, where a proportion of the population are prescribed blood-stage treatment, which allows for asymptomatic infections to be treated. These scenarios do not explore MDA compliance, coverage, and effects of early MDA termination.

## 2. Methods

### 2.1. Transmission model

To capture the transmission dynamics of both *P. falciparum* and *P. vivax*, we use a stochastic agent-based approach for the human population coupled with a deterministic system of ODEs for the mosquito population. Each human agent has their status with respect to both *P. falciparum* and *P. vivax* tracked over time, which allows mixed infections to be captured. The agent-based model is implemented by holding rates constant over discrete time-steps for computational efficiency and for ease of coupling to the ODEs that govern the mosquito population.

Each individual's state is bivariate to specify their state with respect to *P. falciparum* and to *P. vivax*. For each *Plasmodium* species, humans are regarded as being susceptible (*S*), infectious with clinical symptoms (*I*), infectious but asymptomatic (*A*), recovered with no hypnozoites (*R*), recovered with hypnozoites (*L* for latent: not applicable for *P. falciparum*), undergoing blood-stage treatment with no radical cure (*T*), or undergoing treatment with radical cure (*G*). Radical cure is defined as low-dose primaquine (3.5 mg/kg total) administered over 14 days.

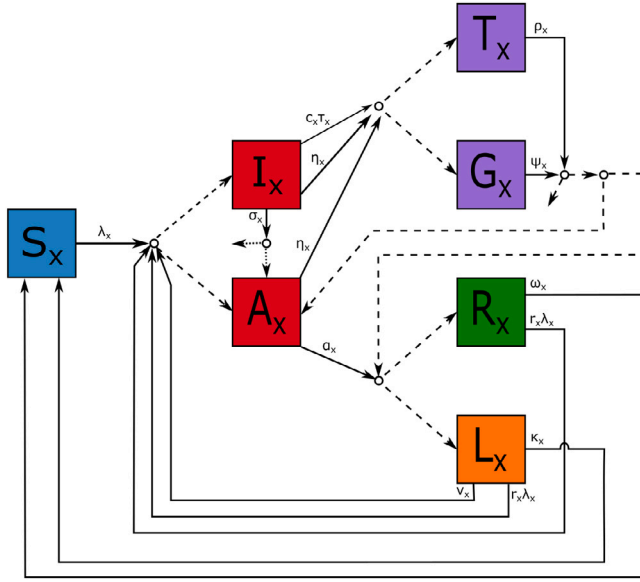


**Fig. 1.** Simplified schematic of the human transmission model for a single parasite species,  $x$ . The model compartments are  $S$  (susceptible),  $I$  (clinical infectious),  $A$  (asymptomatic infectious),  $T$  (undergoing blood-stage treatment),  $G$  (undergoing radical cure),  $R$  (recovered and partially-immune) and  $L$  (latent stage hypnozoites for *P. vivax* only). Solid lines represent rates, the dashed lines probabilities, and the circles designate where a rate is split by probabilities. The probability parameters are not explicitly shown in the figure as, in many cases, the probability of each outcome depends on the current state (for example, the probability of symptoms upon infection is lower for recovered individuals than susceptible individuals).

A simplified schematic of the human transitions are depicted in Fig. 1. Given the large number of connections between states required to describe the transmission and treatment dynamics, the model schematic uses a single line between connectors where multiple transitions apply and does not depict interactions between the species. The full list of possible transition rates and stoichiometries is provided in the Supplementary Table S1.

The dynamics of a human individual infected with type  $x$  malaria are briefly described here for  $x = f$  (*P. falciparum*) and  $v$  (*P. vivax*). Individuals susceptible ( $S$ ) to type  $x$  malaria are infected at rate  $\lambda_x$ . Upon infection they develop clinical symptoms ( $I$ ) with probability  $p_{c,x}$  or are otherwise asymptomatic ( $A$ ). Individuals are symptomatic for a mean duration of  $1/\sigma_x$ , at which point they either become asymptomatic ( $A$ ) or die without treatment with probability  $p_{I,x}$ . The individuals with clinical symptoms may be treated at rate  $c_x \tau_x$ , where  $c_x$  represents availability of treatment and  $\tau_x$  is the rate at which treatment is sought if it is readily available. Individuals with asymptomatic malaria will clear all blood-stage parasites at rate  $\alpha_x$  and, for *P. vivax*, will be left with hypnozoites with probability  $p_{h,v}$ . When an individual with *P. vivax* seeks treatment they are prescribed radical cure ( $G$ ) with probability  $p_{N,x}$ , otherwise they receive blood-stage treatment ( $T$ ).

Any infectious individual may additionally be treated at rate  $\eta_x(t)$  via an intervention program (such as MDA): the form of  $\eta_x(t)$  will be discussed in Section 2.3. When an individual is treated this way they are prescribed radical cure with probability  $p_{M,x}$ , otherwise they receive blood-stage treatment. An individual undergoes treatment for an average of  $1/\psi$  days (14-day primaquine) at which point they may: die with probability  $p_{G,x}$ , remain with asymptomatic blood-stage malaria with probability  $p_{TfP}$ , if  $x = v$  they are left with latent hypnozoites ( $L$ ) with probability  $p_{P,v}$ , otherwise they recover ( $R$ ). Similarly, an individual ends blood-stage treatment after an average of  $1/\rho_x$  days (3-day ACT) at which point they may: die with probability

$p_T$ , remain with asymptomatic blood-stage malaria with probability  $p_{TfA}$ , if  $x = v$  they are left with latent hypnozoites with probability  $p_{A,v}$ , otherwise they recover. Latent stage *P. vivax* infected individuals experience a relapse at rate  $v_v$  or they are reinfected at rate  $\lambda_v r_v$  (where  $r_x$  represents a possible reduction in susceptibility due to anti-parasite immunity) (Doolan et al., 2009). Upon relapse or reinfection from  $L$  the individual experiences clinical malaria with probability  $p_{L,v}$  (where  $p_{L,v} < p_{c,v}$ ). Recovered individuals ( $R$ ) are reinfected with rate  $\lambda_x r_x$  at which point they become a clinical case with probability  $p_{R,x}$  (where  $p_{R,v} < p_{c,v}$ ). In addition to the possibility of relapse or reinfection, recovered and latent individuals lose immunity and hypnozoites at rates  $\omega_x$  and  $\kappa_v$ , respectively, and return to being susceptible.

For individuals with mixed infections, there are several transitions in the model which depend on the individual's state with respect to both species: we refer to these dependencies as species "interactions". When an individual with a mixed infection is treated, they move from states in  $\{I, A, L\}$  to a state in  $\{T, G\}$  for both species (depending on the treatment); this is referred to as "treatment entanglement". Similarly, when a patient stops treatment with respect to one malaria species, they are moved to one of the post-treatment states with respect to the other species. Death with respect to one species will cause a transition to death with respect to the other. The model allows treatment efficacies to vary for mixed infections; however, in this work we have assumed antimalarial efficacy against each species to be equivalent to the efficacy against mono-infections. We model *P. vivax* relapses triggered by the recovery of *P. falciparum* ("triggering") by setting the relapse rate for a person that is recovered ( $R$ ) from *P. falciparum* but has latent stage ( $L$ ) *P. vivax* to be  $\hat{v}_{fv} = z_f v_v$ , where  $z_f > 1$ . The model also allows blood-stage *P. vivax* to be masked by blood-stage *P. falciparum* ("masking") by treating a mixed infection as though it were a *P. falciparum* infection only with probability  $h_v$ . Explicitly, for an individual with *P. falciparum* and *P. vivax* both in states  $I$  or  $A$ , the probability of receiving radical cure is  $p_{N,fv} = h_v p_{N,f} + (1 - h_v) p_{N,v}$ .

## 2.2. Transmission intensity and vector species

The dynamics of the mosquito population are governed by a system of ODEs (presented in the Supplementary Section 2). The mosquitoes follow standard Susceptible–Exposed–Infectious (SEI) dynamics with the addition of a seasonally varying death rate and the ability for mosquitoes to carry and spread mixed infection in a single bite (known as simultaneous inoculation). Asymptomatic individuals tend to have a lower peripheral parasitaemia and therefore were assumed to be less infectious to mosquitoes than individuals with clinical malaria with a relative infectiousness of  $\zeta_{A,x} = 0.1$ . The model represents a context where both *P. falciparum* and *P. vivax* circulate, and the mosquito species present are able to transmit both parasite species allowing mosquitoes to be modelled as a single population that spreads both *P. falciparum* and *P. vivax*.

## 2.3. Treatment scenarios

We simulate three treatment scenarios: current practice, accelerated radical cure, and unified radical cure. In each scenario we assume that when a person tests positive for malaria the species is always identified correctly for mono-infections, since specialised RDTs have been shown to have high sensitivity and specificity, particularly for *P. falciparum* (see, for example, Abba et al. (2014)). The three treatment practices considered are:

1. **Current practice:** Under this scenario, *P. falciparum* and most *P. vivax* cases are prescribed a blood-stage treatment but only 16% of *P. vivax* cases are prescribed radical cure. The low coverage of radical cure was chosen to match the rates reported from a study in Cambodia where radical cure was prescribed conservatively to 16% of detected *P. vivax* cases (Hoyer et al., 2012). That is, the

**Table 1**

Treatments and radical cure coverage by species for each scenario, with an assumed probability of masking of  $h_v = 0.5$ . Here, radical cure (RC) coverage is defined as the probability of receiving radical cure given a detected infection. Treatments ACT, CQ, PQ1 and PQ14 denote a 3-day course of artemisinin-based combination therapy, a 3-day course of chloroquine, a 1-day course of primaquine and a 14-day course of primaquine, respectively.

	Current practice	Accelerated RC	Unified RC
Treatments			
<i>P. falciparum</i>	ACT + PQ1	ACT + PQ1	ACT + PQ14
<i>P. vivax</i>	CQ + PQ14	CQ + PQ14	ACT + PQ14
Mixed	ACT + PQ14	ACT + PQ14	ACT + PQ14
Radical cure coverage (given detected infection)			
<i>P. falciparum</i>	0	0	0.82
<i>P. vivax</i>	0.16	0.82	0.82
Mixed	0.08	0.41	0.82

probability that an individual receives radical cure when being treated for malaria  $x$ , is

$$p_{N,x} = \begin{cases} 0, & \text{for } x = f \\ 0.16, & \text{for } x = v \\ (1 - h_v)0.16, & \text{for } x = fv, \end{cases}$$

where  $h_v$  is the probability that *P. vivax* is masked by *P. falciparum* when the individual is tested.

- Accelerated radical cure:** Under this scenario, any eligible person who is diagnosed with *P. vivax* and returns a G6PD normal RDT is prescribed radical cure with a low-dose 14-day course of primaquine (total dose 3.5 mg/kg) alongside a 3-day course of blood-stage treatment. Anyone who is > 6 months old and is not pregnant or lactating is considered eligible for radical cure. We assume that the G6PD RDTs have a sensitivity of 94% and a specificity of 91% (Ley et al., 2019), 6% of the population have G6PD enzyme activity <30%, 2% of the population are pregnant and/or lactating and 2% of the population are <6 months old. When combined, this means that 18% of people diagnosed with *P. vivax* will be ineligible to receive radical cure (further details are given Supplementary Section 3). The probability of receiving radical cure under this scenario is

$$p_{N,x} = \begin{cases} 0, & \text{for } x = f \\ 0.82, & \text{for } x = v \\ (1 - h_v)0.82, & \text{for } x = fv. \end{cases}$$

- Unified radical cure:** Under this scenario, radical cure is prescribed to any eligible person in whom peripheral parasitaemia is detected, with eligibility as defined and calculated in the accelerated radical cure scenario. The probability of receiving radical cure in this scenario is

$$p_{N,x} = \begin{cases} 0.82, & \text{for } x = f \\ 0.82, & \text{for } x = v \\ 0.82, & \text{for } x = fv. \end{cases}$$

The three treatment scenarios and the probability of receiving radical cure is summarised in Table 1 with an assumed probability of masking of  $h_v = 0.5$ .

For each of the three treatment scenarios we also consider the impact of an MDA intervention where a proportion of the population are given a blood-stage treatment irrespective of infective status, thus allowing a proportion of clinical and asymptomatic blood-stage infections to be treated. We assume that a proportion,  $p$ , of the population are prescribed a blood-stage treatment over a fixed period of time,  $\Delta t = t_2 - t_1$ , so that the treatment rate of an individual with species  $x$  due to MDA is:

$$\eta_x(t) = \begin{cases} \frac{-\ln(1-p)}{\Delta t}, & t \in (t_1, t_2), \\ 0, & \text{otherwise.} \end{cases}$$

We assume that people are not screened for G6PD status nor prescribed radical cure during MDA, based on concerns about haemolytic risks outweighing the benefits in patients who do not have malaria (Ong et al., 2017). That is, the probability that an individual receives radical cure under MDA, given that they are treated for malaria type  $x$  is  $p_{M,x} = 0$  for all  $x$ .

## 2.4. Implementation

We present the impact of different treatment and intervention strategies on the number of malaria cases and deaths in a population of 100,000 individuals over a ten year period, noting that 2030 is the target for malaria elimination in the GMS.

For each treatment and intervention scenario we run 50 model simulations and record the model compartments over time. Given the relatively short time frame, we ignore background human demographic dynamics in our model to reduce computational complexity.

For the *current practice* scenarios we assume that radical cure is prescribed conservatively and does not increase the risk of haemolysis (as a best case scenario). To account for haemolytic risk in the *accelerated radical cure* and *unified radical cure* scenarios we increase the probability of death by  $5 \times 10^{-6}$  for patients administered primaquine and the probability of radical cure failure by  $5 \times 10^{-4}$  (details on these values are given in Supplementary Section 3).

For the MDA intervention, we assume that half of the population receive blood-stage treatment over a 30 day period. The MDA is rolled out twice yearly, before and after the annual peak in transmission.

Some parameter values were based on expert elicitation or a limited evidence base, and some parameter estimates vary greatly between studies. Accordingly, the scenarios here should not be interpreted as forecasts of malaria cases and deaths in the GMS region over the next 10 years. The scenarios presented here are indicative of population dynamics of multi-species infections over time that accommodates interaction between *P. falciparum* and *P. vivax* infections and expected trends in the impacts of different interventions. All parameters and initial conditions are given in Supplementary Tables S2 and S3.

We performed a sensitivity analysis on the model, in which each model parameter was modified separately and the relative change in model outputs recorded. To implement the sensitivity analysis, we considered the baseline value of each parameter (given in Tables 2 and 3) and ran simulations with the parameter scaled down to 80% and up to 120% while all other parameters remained fixed. If scaling a probability parameter up to 120% compared to baseline led to a probability being greater than 1 the value was instead held at 1. Similarly, the relative susceptibility of partially-immune individuals compared to susceptible individuals was not scaled up, so as not to exceed 1. For each set of parameter values, 50 repeats of the simulation were conducted and various outputs were recorded, including: the total number of *P. falciparum* infections, *P. vivax* infections, clinical *P. falciparum* infections, clinical *P. vivax* infections, *P. vivax* relapses, deaths, blood-stage treatments administered, and radical cure treatments administered. The implementation of the model in Python 3.9.4 and other supplementary material are provided on GitHub at <https://github.com/jnwalker2/multispecies-malaria-model>.

## 3. Results

### 3.1. Scenario modelling

Results for the scenario analysis are presented in terms of the number of infectious individuals over time and cumulative outcomes over the simulation horizon in Figs. 2 and 3.

Fig. 2 depicts the total number of infectious individuals in the population over time (the median, minimum and maximum of the 50 simulations) and figures showing all model compartments through time are presented in Supplementary Figures S2 and S3. The different



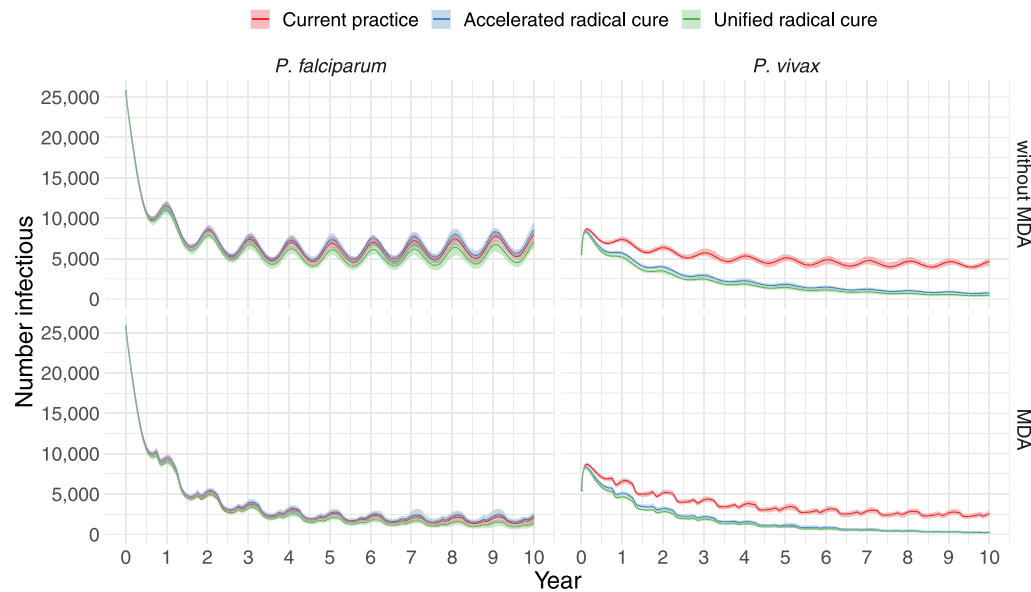


Fig. 2. Infections over 10 years for *P. falciparum* (left panels) and *P. vivax* (right panels) with clinical treatment only (top row), and mass drug administration (MDA) (bottom row).

treatment strategies had little effect on the prevalence of *P. falciparum*, with the unified treatment scenario resulting in a marginally lower prevalence of *P. falciparum*. For *P. vivax* increasing the coverage of radical cure has a large impact on the prevalence of *P. vivax*, which appears to be approaching elimination towards the end of the time period. Meanwhile, the MDA intervention greatly reduced the prevalence of *P. falciparum* but had less of an effect on *P. vivax*. No scenarios led to elimination of malaria over the ten year period, although elimination may have been achieved over a longer time-frame. We note that uncertainty ranges in Fig. 2 reflect model uncertainty for the baseline parameter set, whereas, the additional effect of parameter uncertainty is captured in the sensitivity analysis. The uncertainty bounds are relatively narrow, indicating that stochastic effects from the model are negligible until the population is closer to elimination. Incorporating parameter uncertainty will substantively widen these bounds.

Fig. 3 shows boxplots of the cumulative number of infections and deaths by species over the 10 year period. The unified treatment strategy with G6PD testing of all individuals resulted in fewer infections and fewer overall deaths, despite the increased risk of haemolysis from radical cure. The accelerated radical cure approach approximately halved *P. vivax* infections but resulted in a small increase in *P. falciparum* infections, this increase is likely due to a reduction in the prevalence of mixed infections, which are more likely to be detected than mono-infections, inadvertently causing a reduction in the detection rate of *P. falciparum*.

### 3.2. Sensitivity analysis

In Fig. 4, the results of the sensitivity analysis are presented in terms of the ten most influential parameters on cumulative infections (including clinical and asymptomatic cases). Sensitivity analyses with respect to all parameters and other outcomes are given in Supplementary Figure S4. These figures present the mean, minimum and maximum relative outcome compared to the baseline over 50 simulations, for each parameter set and orders them based on their relative sensitivity (in terms of absolute difference between the 80% and 120% scenarios).

In Fig. 4 we see that *P. falciparum* and *P. vivax* infections were most sensitive to many of the vector-related parameters, including: the bite rate ( $b$ ), the death rate of mosquitoes ( $\delta_0$ ), the probability of transmission given an infectious bite (from humans to mosquitoes and vice versa,  $\epsilon_{M,x}$  and  $\epsilon_{H,x}$ ) and the rate at which exposed mosquitoes become

infectious ( $\gamma_x$ ). The spread of mosquito-borne infectious diseases are well known to be sensitive to these parameters (Chitnis et al., 2008).

Aside from the vector-related parameters, we identified several important human-related parameters, including: the relative infectiousness of asymptomatic carriers ( $\zeta_{A,x}$ ), the relative susceptibility of partially-immune individuals ( $r$ ), the rate at which asymptomatic infections are cleared ( $\alpha_x$ ), the rate of treatment seeking ( $\tau_x$ ), and accessibility of treatment ( $c$ ). The parameters  $\zeta_{A,x}$  and  $\alpha_x$  determine the expected number of secondary infections generated by asymptomatic individuals. The parameter  $r$  is related to anti-parasite immunity, it represents a possible lower rate of infection in recovered individuals. The parameters  $\tau_x$  and  $c$  determine the rate at which clinical cases seek treatment and the probability that they receive treatment for malaria.

In addition to the parameters that were influential on cumulative infections of both species, *P. vivax* infections were sensitive to the probability that hypnozoites are cleared when blood-stage parasites are cleared without treatment ( $p_h$ ). This emphasises the contribution of relapses in the overall *P. vivax* malaria burden.

Other model outcomes (clinical infections, total deaths, total relapses, total treatments received) were broadly sensitive to the same model parameters without any additions or omissions (see Supplement Figure 4 for details). Small differences in relative sensitivity between measuring cumulative infections versus clinical infections were largely centred on the parameters having to do with the proportions immune expected to develop clinical malaria upon reinfection (that is,  $p_R$  for *P. falciparum* and  $p_c$  for *P. vivax*).

### 4. Discussion

Capturing the dynamics of multiple malaria species concurrently is policy-relevant but has drawn little attention to date. In this paper, we have developed a model of sufficient complexity to capture these dynamics, demonstrating how it can be used to inform health policy. Our model incorporates the dynamics of both *P. falciparum* and *P. vivax* in a way that captures masking, treatment entanglement and triggering interactions of the species. This is the second multi-species model which meaningfully captures dependencies between *P. falciparum* and *P. vivax* (Silal et al., 2019) and is the only stochastic, agent-based model to do so. The stochasticity in our approach makes it particularly well suited to model *P. falciparum* and *P. vivax* in low transmission settings, small populations, or as malaria is approaching elimination. The model

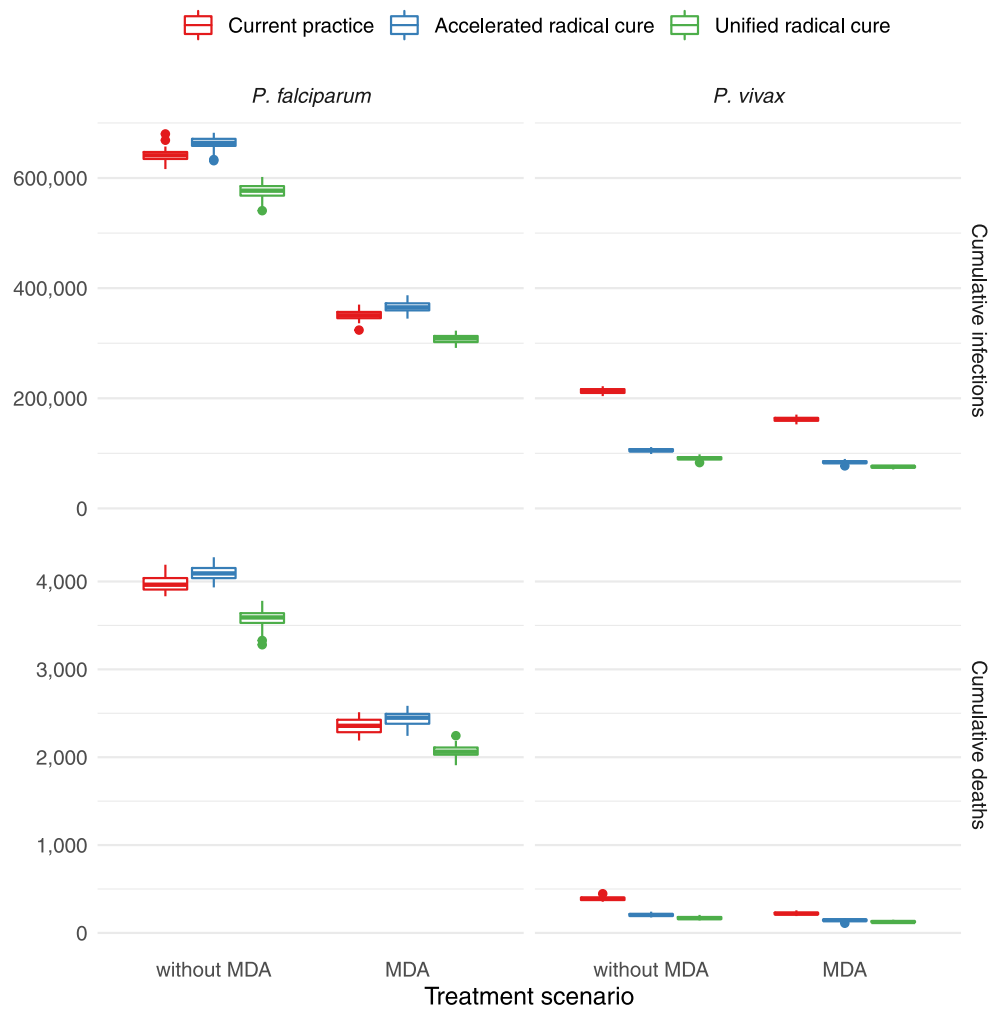


Fig. 3. Cumulative infections and deaths over a 10 year period with and without mass drug administration (MDA) for *P. falciparum* (left panels) and *P. vivax* (right panels).

also has fewer compartments, and fewer parameters, than the only other model with similar features (Sital et al., 2019), making our model more readily parameterised. The discrete stochastic modelling approach is well suited to a complex multi-species epidemic process like this because there are many different states that an individual can be in, and therefore the number of people in a given state may be too small to reasonably be represented by a continuous deterministic model.

Our scenario analysis explored the effect of different proportions of coverage with radical cure treatment, assuming that individuals were screened for G6PD deficiency prior to treatment. The scenario analysis showed that a unified radical cure strategy can reduce the prevalence of malaria cases and deaths overall, even when accounting for the increased risk of death due to haemolysis under radical cure. Radical cure is effective because it blocks transmission, kills blood-stage parasites, and kills dormant hypnozoites. A unified radical cure strategy avoids issues associated with masking when administering targeted treatment, allows for a consistent protocol for malaria treatment, and does not require the speciation of malaria prior to treatment. Not many countries are currently prescribing primaquine to *P. vivax* patients due to concerns about the cost of G6PD screening (Thriemer et al., 2017), so it may be even more challenging for this to be extended to *P. falciparum* patients. Accordingly, our multi-species model has enabled us to explore the impact on incidence and deaths under a unified radical cure strategy.

Modelling a twice-yearly MDA intervention allowed us to assess the additional impact that could be achieved by the blood-stage treatment

of asymptomatic infections as a means to reduce malaria burden. We found that MDA is an effective way to reduce prevalence, but it will not necessarily lead to elimination if coverage is too low. This is in line with a report from WHO, based on a systematic review of 270 literature reports, which states that for MDA to be effective, at least 80% of the population should be treated (WHO, 2015). Achieving those levels of population coverage may be difficult due to issues with compliance. Due to safety concerns about treating individuals with G6PD deficiency with radical cure, only MDA with blood-stage treatment was considered. Consequently we found that MDA decreased *P. falciparum* prevalence but had less of an effect on *P. vivax* prevalence. Targeted interventions may allow radical cure to be administered *en masse* (such as focal screen and treat, or mass screen and treat) (WHO, 2015). Our modelling framework easily allows these other kinds of interventions to be incorporated through the time-varying treatment function,  $\eta_x(t)$ .

The modelling framework has some limitations, including that immunity from multiple infections, age-stratification, and non-pharmaceutical interventions (e.g. insecticide treated nets and indoor residual spray) were not explicitly modelled. These can to some extent be factored into model parameters, for example, reducing the bite rate and increasing the mosquito death rate to account for non-pharmaceutical interventions. The model did not factor in treatment-resistant strains, though this can similarly be captured by increasing the probability of treatment failure under the strong assumption that

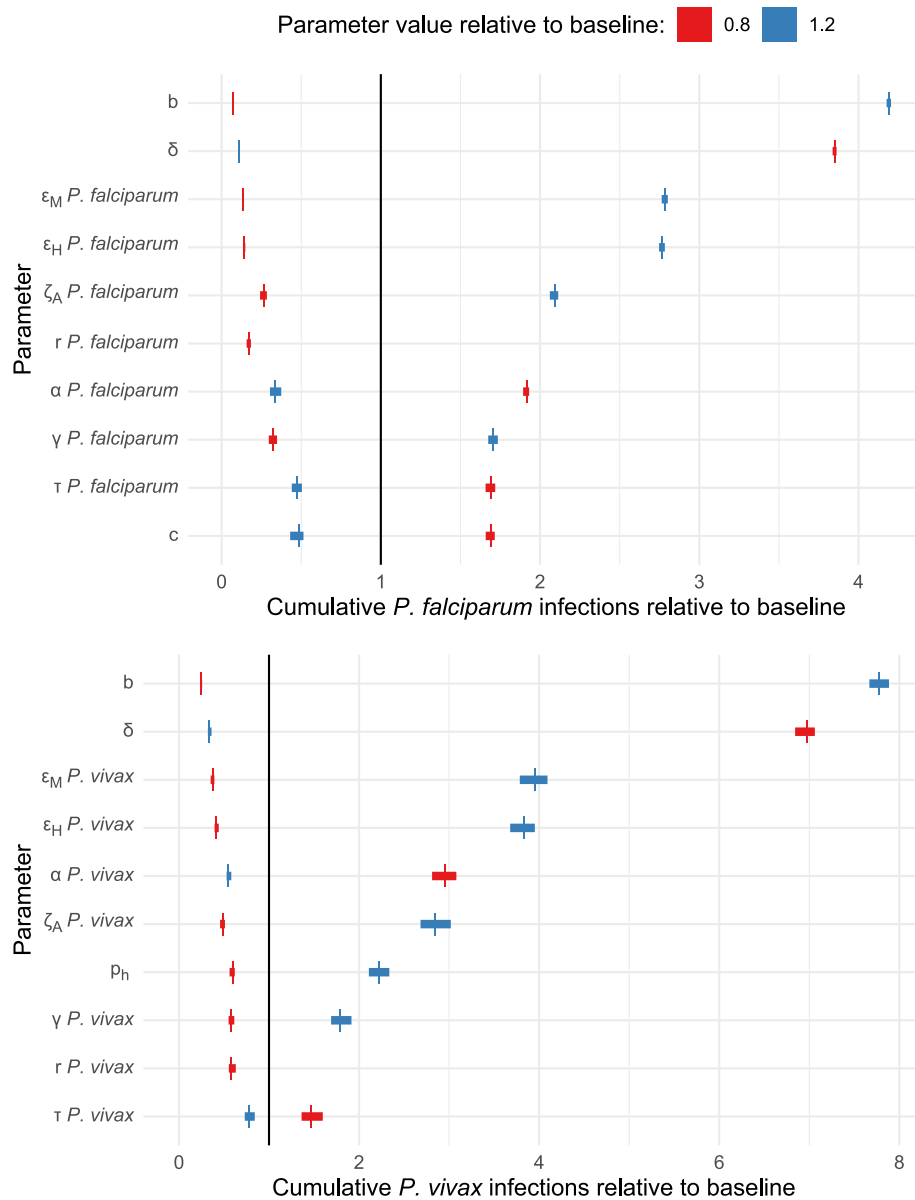


**Fig. 4.** Sensitivities of *P. falciparum* (top) and *P. vivax* (bottom) cumulative infections with respect to varying model parameters. These are presented in terms of the mean relative outcome, compared to baseline, when each parameter is scaled by 0.8 and 1.2. Red and blue vertical lines represent the mean outcomes relative to baseline given a parameter scaling of 0.8 and 1.2, respectively. Error bars represent the minimum and maximum relative outcome, compared to baseline. Each minimum, mean and maximum calculated from 50 simulations.

the level of resistance is fixed. This study was limited in its exploration of MDA compliance, coverage, and effects of early MDA termination, the latter of which is well known to lead to resurgence if malaria is not eliminated. This was intentionally left for future work with the focus of this study primarily being on the interactions between species and how different treatment strategies affect the two species in this framework.

The sensitivity analysis shows that, although the model has many parameters, the outputs are sensitive to relatively few parameters. The most sensitive parameters for both species were those related to vector-dynamics, the bite rates, transmission probabilities, mosquito death rate and the infectious period of mosquitoes, which are well known to be influential for mosquito-spread diseases (Chitnis et al., 2008). Additionally, the relative infectiousness of asymptomatic individuals ( $\zeta_{A,x}$ ), the rate at which asymptomatic infections are cleared ( $\alpha_x$ ), the relative susceptibility of partially-immune individuals ( $r$ ), the rate of treatment seeking ( $\tau$ ) and accessibility of treatment ( $c$ ) were all found

to be influential. Note that  $\tau$  and  $c$  determine the proportion of clinical infections that go untreated and become asymptomatic. Further,  $\zeta_{A,x}$  and  $\alpha_x$  determine the expected number of secondary infections generated by asymptomatic individuals. These sensitivities highlight how important asymptomatic individuals can be in driving malaria burden and the need for interventions that target asymptomatic infections, such as MDA (explored in this work) or better diagnostics that can detect infections with low level parasitaemia.

The number of *P. vivax* infections was sensitive to the probability of asymptomatic carriers naturally clearing hypnozoites, reinforcing the notion that relapses contribute significantly to malaria burden, as has been shown empirically in an analysis of 68,361 patients in Indonesia (Dini et al., 2020). It is worth noting that since we performed a one-dimensional sensitivity analysis, the results should only be interpreted as the output sensitivity with respect to each parameter in

isolation, and not interpreted as a full quantification of model output variation. A full probabilistic sensitivity analysis is appropriate for assessing output uncertainty, particularly if using the model to inform public health policy.

The simulations in our scenario analyses show behaviour comparable to parts of the GMS with parameters consistent with literature and expert elicitation. Many of the model parameters are location-specific such as the bite rate, relative infectiousness of asymptomatic carriers, probability of death from radical cure and the initial model state. Future work will develop a statistical framework for fitting this model, so that it can be applied to specific endemic settings where parameters may differ substantially. The complexity of the multi-species model poses a challenge to jointly fitting all model parameters because of the high dimension of the parameter space and the run time, which was on the scale of minutes for a single simulation over 10 years. Optimised approximate Bayesian inference methods such as Bayesian Optimisation for Likelihood-Free Inference (BOLFI) and Likelihood-Free Inference by Ratio Estimation (LFIRE) may provide solutions to both of these challenges (Gutmann et al., 2016; Thomas et al., 2022). If the run time of the stochastic model becomes prohibitive for inference, as may be the case when applied to larger populations with high prevalence (where capturing small fluctuations in low numbers is less important), a deterministic or hybrid model equivalent could be applied instead.

This modelling framework provides the basis for future malaria modelling studies to evaluate the impact of integrated malaria control packages in settings where *P. falciparum* and *P. vivax* are co-endemic. In particular, parameters in the model can be adjusted to consider vector control measures and to evaluate other treatments, such as single-dose tafenoquine, high-dose 7-day primaquine, and triple ACTs. The multi-species malaria model was developed in a way that enables economic analyses through the evaluation of the impact of different malaria control activities on outcomes for individuals, such as the different treatment strategies assessed here. In the future, costs and quality of life metrics can be evaluated alongside the impact on cases and deaths. For example, this model could be used to identify under which circumstances a unified treatment for malaria would be cost-effective. Lastly, the modelling framework could be expanded to include other species of malaria, such as zoonotic *P. knowlesi*.

## Role of the funding source

ACREME funded the salary of RIH, and contributed to the costs of data cleaning and organisation by PN and the CNM.

## CRediT authorship contribution statement

**C.R. Walker:** Software, Conceptualisation, Methodology, Writing. **R.I. Hickson:** Software, Conceptualisation, Methodology, Writing. **E. Chang:** Software, Visualisation. **P. Ngor:** Data curation. **S. Sovannaroeth:** Data curation. **J.A. Simpson:** Conceptualisation. **D.J. Price:** Conceptualisation, Visualisation. **J.M. McCaw:** Conceptualisation. **R.N. Price:** Conceptualisation. **J.A. Flegg:** Project administration, Conceptualisation. **A. Devine:** Project administration, Conceptualisation, Writing.

## Declaration of competing interest

None.

## Data availability

Source code is available from: <https://github.com/jnwalker2/multi-species-malaria-model>

## Acknowledgements

This work is supported in part by the Australian Centre for Research Excellence in Malaria Elimination (ACREME), funded by the NHMRC (1134989). J.A. Simpson is funded by an Australian National Health and Medical Research Council of Australia (NHMRC) Investigator Grant (1196068). R.N. Price is a Wellcome Trust Senior Fellow in Clinical Science (200909). This research was funded in whole, or in part, by the Wellcome Trust (200909). For the purpose of open access, the author has applied a CC BY public copyright licence to any Author Accepted Manuscript version arising from this submission. J.M. McCaw's research is supported by the ARC (DP170103076, DP210101920) and ACREME. J.A. Flegg's research is supported by the ARC (DP200100747, FT210100034). A. Devine's research is supported by National Health and Medical Research Council of Australia (NHMRC) (APP1132975). The contents of the published material are solely the responsibility of the individual authors and do not reflect the views of NHMRC. A. Devine and D.J. Price's research are supported by DFAT. C.R. Walker's research is supported by the Andrew Sisson support package.

## Appendix A. Supplementary data

Supplementary material related to this article can be found online at <https://doi.org/10.1016/j.epidem.2023.100687>.

## References

- Abba, Katharine, Kirkham, Amanda J., Oliaro, Piero L., Deeks, Jonathan J., Donegan, Sarah, Garner, Paul, Takwoingi, Yemisi, 2014. Rapid diagnostic tests for diagnosing uncomplicated non-falciparum or *Plasmodium vivax* malaria in endemic countries. *Cochrane Database Syst. Rev.* 2014 (12), CD011431.
- Adekunle, Adeshina I., Pinkevych, Mykola, McGready, Rose, Luxemburger, Christine, White, Lisa J., Nosten, François, Cromer, Deborah, Davenport, Miles P., 2015. Modeling the dynamics of *Plasmodium vivax* infection and hypnozoite reactivation in vivo. *PLoS Negl. Trop. Dis.* 9 (3), e0003595.
- Aguiar, Ricardo, Ferreira, Marcelo U., Gabriela M. Gomes, M., 2012. Modeling the effects of relapse in the transmission dynamics of malaria parasites. *J. Parasitol. Res.* 2012.
- Ashton, Ruth A., Kefyalew, Takele, Tesfaye, Gezahegn, Counihan, Helen, Yadeta, Dامتew, Cundill, Bonnie, Reithinger, Richard, Kolaczinski, Jan H., 2010. Performance of three multi-species rapid diagnostic tests for diagnosis of *Plasmodium falciparum* and *Plasmodium vivax* malaria in Oromia Regional State, Ethiopia. *Malar. J.* 9 (1), 297.
- Carrara, Verena I., Lwin, Khin Maung, Phyto, Aung Pyae, Ashley, Elizabeth, Wiladphaingern, Jacher, Sriprawat, Kanlaya, Rijken, Marcus, Boel, Machteld, McGready, Rose, Proux, Stephane, Chu, Cindy, Singhasivanon, Pratap, White, Nicholas, Nosten, François, 2013. Malaria burden and artemisinin resistance in the mobile and migrant population on the Thai–Myanmar border, 1999–2011: An observational study. *PLoS Med.* 10 (3), e1001398.
- Chhim, Srean, Piola, Patrice, Housen, Tambri, Herbreteau, Vincent, Tol, Bunkea, 2021. Malaria in Cambodia: A retrospective analysis of a changing epidemiology 2006–2019. *Int. J. Environ. Res. Public Health* 18 (4).
- Chitnis, Nakul, Hyman, James M., Cushing, Jim M., 2008. Determining important parameters in the spread of malaria through the sensitivity analysis of a mathematical model. *Bull. Math. Biol.* 70 (5), 1272.
- Commons, Robert J., Simpson, Julie A., Thriemer, Kamala, Hossain, Mohammad S., Douglas, Nicholas M., Humphreys, Georgina S., Sibley, Carol H., Guerin, Philippe J., Price, Ric N., 2019. Risk of *Plasmodium vivax* parasitaemia after *Plasmodium falciparum* infection: a systematic review and meta-analysis. *Lancet Infect. Dis.* 19 (1), 91–101.
- Dini, Saber, Douglas, Nicholas M., Poespoprodjo, Jeanne Rini, Kenangalem, Enny, Sugiarto, Paulus, Plumb, Ian D., Price, Ric N., Simpson, Julie A., 2020. The risk of morbidity and mortality following recurrent malaria in Papua, Indonesia: a retrospective cohort study. *BMC Med.* 18 (1), 1–12.
- Doolan, Denise L., Dobaño, Carlota, Kevin Baird, J., 2009. Acquired immunity to malaria. *Clin. Microbiol. Rev.* 22 (1), 13–36.
- Douglas, Nicholas M., John, George K., von Seidlein, Lorenz, Anstey, Nicholas M., Price, Ric N., 2012. Chemotherapeutic strategies for reducing transmission of *Plasmodium vivax* malaria. *Adv. Parasitol.* 80, 271–300.
- Gosling, Roly D., Whittaker, Maxine, Gueye, Cara Smith, Fullman, Nancy, Baquilod, Mario, Kusriastuti, Rita, Feachem, Richard G.A., 2012. Malaria elimination gaining ground in the Asia Pacific. *Malar. J.* 11 (1), 1–3.
- Gutmann, Michael U., Cor, Jukka, er, 2016. Bayesian optimization for likelihood-free inference of simulator-based statistical models. *J. Mach. Learn. Res.* 17 (125), 1–47.



- Hossain, Mohammad S., Commons, Robert J., Douglas, Nicholas M., Thriemer, Kamala, Alemayehu, Bereket H., Amaratunga, Chanaki, Anvikar, Anupkumar R., Ashley, Elizabeth A., Asih, Puji B.S., Carrara, Verena L., Lon, Chanthap, D'Alessandro, Umberto, Davis, Timothy M.E., Dondorp, Arjen M., Edstein, Michael D., Fairhurst, Rick M., Ferreira, Marcelo U., Hwang, Jimee, Janssens, Bart, Karunajeewa, Harin, Kiechel, Jean R., Ladeia-Andrade, Simone, Laman, Moses, Mayxay, Mayfong, McGready, Rose, Moore, Brioni R., Mueller, Ivo, Newton, Paul N., Thuy-Nhien, Nguyen T., Noedl, Harald, Nosten, Francois., Phyo, Aung P., Poespoprodjo, Jeanne R., Saunders, David L., Smithuis, Frank, Spring, Michele D., Stepniewska, Kasia, Suon, Seila, Suputtamongkol, Yupin, Syafruddin, Din, Tran, Hien T., Valecha, Neena, Herp, Michel Van, Vugt, Michele Van, White, Nicholas J., Guerin, Philippe J., Simpson, Julie A., Price, Ric N., 2020. The risk of *Plasmodium vivax* parasitaemia after p. falciparum malaria: An individual patient data meta-analysis from the Worldwide Antimalarial Resistance Network. *PLoS Med.* 17 (11), 1–26.
- Hoyer, Stefan, Nguon, Sokomar, Kim, Saorin, Habib, Najibullah, Khim, Nimol, Sum, Sarorn, Christophel, Eva-Maria, Borge, Steven, Thomson, Andrew, Kheng, Sim, Chea, Nguon, Yok, Sovann, Top, Samphornarann, Ros, Seyha, Sophal, Uth, Thompson, Michelle M., Mellor, Steve, Arie, Frédéric, Witkowski, Benoit, Yeang, Chhiang, Yeung, Shunmay, Duong, Socheat, Newman, Robert D., Menard, Didier, 2012. Focused screening and treatment (FSAT): A PCR-based strategy to detect malaria parasite carriers and contain drug resistant p. falciparum, Pailin, Cambodia. *PLoS One* 7 (10), 1–12.
- Kenangalem, Enny, Poespoprodjo, Jeanne Rini, Douglas, Nicholas M., Burdam, Faustina Helena, Gdeumana, Ketut, Chalfein, Ferry, Prayoga, Thio, Franciscus, Devine, Angela, Marfurt, Jutta, Waramori, Govert, Yeung, Shunmay, Noviyanti, Rintis, Penttinen, Pasi, Bangs, Michael J., Sugiarto, Paulus, Simpson, Julie A., Soenarto, Yati, Anstey, Nicholas M., Price, Ric N., 2019. Malaria morbidity and mortality following introduction of a universal policy of artemisinin-based treatment for malaria in Papua, Indonesia: A longitudinal surveillance study. *PLoS Med.* 16 (5), 1–23.
- Landier, Jordi, Parker, Daniel M., Thu, Aung Myint, Lwin, Khin Maung, Delmas, Gilles, Nosten, François H., Andolina, Chiara, Aguas, Ricardo, Ang, Saw Moe, Aung, Ei Phyo, Baw, Naw Baw, Be, Saw Aye, B'Let, Saw, Bluh, Hay, Bonnington, Craig A., Chaumeau, Victor, Chirakiratinant, Miasa, Cho, Win Cho, Christensen, Peter, Corbel, Vincent, Day, Nicholas P.J., Dah, Saw Hsa, Delmas, Gilles, Dhorda, Mehul, Dondorp, Arjen M., Gaudart, Jean, Gornawun, Gornpan, Haohankhunnatham, Warat, Hla, Saw Kyaw, Hsel, Saw Nay, Htoo, Gay Nay, Htoo, Saw Nay, Imwong, Mallika, John, Saw, Kajeechiwa, Ladda, Kerecharoen, Lily, Kittiphanakun, Praphan, Kittitawee, Keerati, Konghahong, Kamonchanok, Khin, Saw Diamond, Kyaw, Saw Win, Landier, Jordi, Ling, Clare, Lwin, Khin Maung, Lwin, Khine Shwe War, Ma, Naw K' Yin, Marie, Alexandra, Maung, Cynthia, Marta, Ed, Minh, Myo Chit, Miotto, Olivo, Moo, Paw Khu, Moo, Ku Ler, Moo, Merry, Na, Naw Na, Nay, Mar, Nosten, François H., Nosten, Suphak, Nyo, Slight Naw, Oh, Eh Kalu Shwe, Oo, Phu Thit, Oo, Tun Pyit, Parker, Daniel M., Paw, Eh Shee, Phumiya, Choochai, Phyo, Aung Pyae, Pilaseng, Kasiha, Proux, Stéphane, Rakthinhong, Santisuk, Ritwongsakul, Wannee, Salathibuppha, Kloi, Santirad, Armon, Sawasdechai, Sunisa, von Seidlein, Lorenz, Shee, Paw Wah, Shee, Paw Bway, Tangseefa, Decha, Thu, Aung Myint, Thwin, May Myo, Tun, Saw Win, Wanachaloemle, Chode, White, Lisa J., White, Nicholas J., Wiladphaingern, Jacher, Win, Saw Nyunt, Yee, Nan Lin, Yuwapan, Daraporn, 2018. Effect of generalised access to early diagnosis and treatment and targeted mass drug administration on *Plasmodium falciparum* malaria in Eastern Myanmar: an observational study of a regional elimination programme. *Lancet* 391 (10133), 1916–1926.
- Ley, Benedikt, Satyagraha, Ari Winasti, Rahmat, Hisni, von Fricken, Michael E., Douglas, Nicholas M., Pfeffer, Daniel A., Espino, Fe, von Seidlein, Lorenz, Henriques, Gisela, Oo, Nwe Nwe, Menard, Didier, Parikh, Sunil, Banccone, Germana, Karahalios, Amalia, Price, Ric N., 2019. Performance of the Access Bio/CareStart rapid diagnostic test for the detection of glucose-6-phosphate dehydrogenase deficiency: A systematic review and meta-analysis. *PLoS Med.* 16, 1–15.
- Lin, Jessica T., Bethell, Delia, Tyner, Stuart D., Lon, Chanthap, Shah, Naman K., Saunders, David L., Sriwichai, Sabaithip, Khemawoot, Phisit, Kuntawunggin, Worachet, Smith, Bryan L., Noedl, Harald, Schaecher, Kurt, Socheat, Duong, Se, Youry, Meshnick, Steven R., Fukuda, Mark M., 2011. *Plasmodium falciparum* gametocyte carriage is associated with subsequent *Plasmodium vivax* relapse after treatment. *PLoS One* 6 (4), 1–8.
- Mandal, Sandip, Sarkar, Ram, Sinha, Somdatta, 2011. Mathematical models of malaria - a review. *Malar. J.* 10 (1), 202.
- Ong, Ken Ing Cherng, Kosugi, Hodaka, Thoeun, Sophea, Araki, Hitomi, Thandar, Moe Moe, Iwagami, Moritoshi, Hongvanthong, Bouasy, Brey, Paul T., Kano, Shigeyuki, Jimba, Masamine, 2017. Systematic review of the clinical manifestations of glucose-6-phosphate dehydrogenase deficiency in the Greater Mekong Subregion: implications for malaria elimination and beyond. *BMJ Glob. Health* 2 (3), e000415.
- Poespoprodjo, Jeanne Rini, Burdam, Faustina Helena, Candrawati, Freis, Ley, Benedikt, Meagher, Niamh, Kenangalem, Enny, Indrawanti, Ratni, Triant, Leily, Thriemer, Kamala, Price, David J., et al., 2022. Supervised versus unsupervised primaquine radical cure for the treatment of falciparum and vivax malaria in Papua, Indonesia: a cluster-randomised, controlled, open-label superiority trial. *Lancet Infect. Dis.* 22 (3), 367–376.
- Pongsumpun, Puntani, Tang, I-Ming, 2008. Mathematical model for the transmission of *P. falciparum* and *P. vivax* malaria along the Thai-Myanmar border. *Int. J. Biol. Life Sci.* 3.
- Pongsumpun, Puntani, Tang, I-Ming, 2010. Impact of cross-border migration on disease epidemics: case of the *P. falciparum* and *P. vivax* malaria epidemic along the Thai-Myanmar border. *J. Biol. Systems* 18 (01), 55–73.
- Price, Ric N., Commons, Robert J., Battle, Katherine E., Thriemer, Kamala, Mendis, Kamini, 2020. *Plasmodium vivax* in the era of the shrinking p. falciparum map. *Trends Parasitol.* 36 (6), 560–570.
- Silal, Sheetal Prakash, Shretta, Rima, Celhay, Olivier J., Chris, Saralamba, Sompob, Erwin Gran Mercado, Maude, Richard James, White, Lisa Jane, 2019. Malaria elimination transmission and costing in the Asia-Pacific: a multi-species dynamic transmission model. *Wellcome Open Res.* 4 (62).
- Smith, Neal R., Trauer, James M., Gambhir, Manoj, Richards, Jack S., Maude, Richard J., Keith, Jonathan M., Flegg, Jennifer A., 2018. Agent-based models of malaria transmission: a systematic review. *Malar. J.* 17 (1), 299.
- Thomas, Owen, Dutta, Ritabrata, Corander, Jukka, Kaski, Samuel, Gutmann, Michael U., 2022. Likelihood-free inference by ratio estimation. *Bayesian Anal.* 17 (1), 1–31.
- Thriemer, Kamala, Ley, Benedikt, Bobogare, Albino, Dysoley, Lek, Alam, Mohammad Shafiu, Pasaribu, Ayodhia P., Sattabongkot, Jetsumon, Jambert, Elodie, Domingo, Gonzalo J., Commons, Robert, et al., 2017. Challenges for achieving safe and effective radical cure of *Plasmodium vivax*: a round table discussion of the APMEN Vivax Working Group. *Malar. J.* 16 (1), 1–9.
- WHO, 2015. Meeting Report of the Evidence Review Group on Mass Drug Administration, Mass Screening and Treatment and Focal Screening and Treatment for Malaria. World Health Organization, Geneva.
- WHO, 2020. World Malaria Report 2020. Technical Report, World Health Organization, Geneva.
- WHO, 2021. World Malaria Report 2021. Technical Report, World Health Organization, Geneva.
- WHO, 2022. WHO Guidelines for Malaria 2022. World Health Organization, Geneva.